8. ANKARA INTERNATIONAL AEROSPACE CONFERENCE **AIAC-2015-163**
10-12 September 2015 - METU, Ankara TURKEY

ICE ACCRETION PREDICTION ON HORIZONTAL AXIS WIND TURBINE BLADES

Serkan Özgen* , Özcan Yırtıcı † and İsmail H. Tuncer ‡
Middle East Technical University
Ankara, Turkey

ABSTRACT

Ice accretion on the blades change the initial shape and this cause alteration in the aerodynamic characteristic of the blades. The objective of this study is to predict the shape of the iced blade sections of the turbine blade under atmospheric icing conditions. The obtained results are verified with experimental and numerical ice shapes reported in the literature. In all the cases studied, the current numerical tool yields results that are in fair agreement with the compared results and can be used to predict ice accretion on wind turbine's blades under atmospheric icing conditions.
.

INTRODUCTION

The green energy has been significant since the global warming has caused climate changes in recent years. Therefore utilizing of wind energy has gained importance and installation of wind turbines in the world has been increasing in a steady manner. About three percent of the world's electricity is delivered by wind power. This share is expected to grow to 7.3 percent by 2018 according to Navigant Research [Navigant Research, 2015]. Wind resources in cold climate regions and mountainous areas are typically good and making them attractive for wind energy. However especially in winter, the wind turbines are exposed to heavy atmospheric icing conditions. In the horizontal axis wind turbines, aerodynamic performance losses are similar to that observed by wings and helicopter rotors under icing conditions [Jasinski, 1998]. Atmospheric icing causes power losses since ice accretion on blades changes the clean blade aerodynamic characteristics and creates instrument or controller errors on wind turbines. The amount of wind power losses depend on the amount of ice accumulation on the blades, blade design and turbine control. Therefore, wind power estimation plays an important role on wind farm selection as the investment cost comes dearly.

Aerodynamic performance degradation can reduce the power coefficient in the range of $20-50\%$ [Talhaug, 2007] and the annual energy production (AEP) by up to 17% [Barber , 2011]. For this reason, the international energy agency (IEA) announced Annex XIX: "Wind Energy in Cold Climates"

*Prof. in Aerospace Engineering Department, Email: sozgen@ae.metu.edu.tr
†Gra. in a Aerospace Engineering Department, Email: oyirtici@ae.metu.edu.tr
‡Prof. in a Aerospace Engineering Department, Email: tuncer@ae.metu.edu.tr

to predict better the effect of ice accretion on energy production [IEA Wind , 2015]. In order to prevent or mitigate icing effects on wind turbine active or passive anti-icing and de-icing systems (ADIS) can be used, but few are available on the market. ADIS are generally based on heating, therefore wind turbines need more power to operate. Although early power consumptions of ADIS electrical heating were $\approx$ 25 % of the nominal power output of the given turbine, with the advances in technology this consumption is reduced to $\approx$ 2 % of nominal power output. Nowadays ADIS use up 4 % of the annual energy production depending on icing severity [Parent , 2011]. Icing modeling can aid in the positioning of ADIS to reduce energy consumption needed to operate these devices.

Figure 1: GE 2.5-100 wind turbine encounters fog in July, 2015, Samandağ, Turkey.

In order to maximize energy production from the turbine which is operating under icing conditions performance losses needed to be predicted. Fluid flow simulation that predicts ice formation on turbine blades can help maintain safety, reduce performance losses and decrease weight.

METHOD

Icing modeling makes it possible to obtain data for generating ice shapes for geometries like aircraft, transmission line wires, etc. under a wide range of simulation conditions. Icing module is used to predict icing shape geometry at given blade sections on the wind turbine blade. The main inputs to this module are blade section geometry, flow conditions (free stream velocity, angle of attack, etc.) and weather conditions (temperature, MVD, LWC, exposure time, etc.). The main outputs are sectional ice shape geometry and corresponding aerodynamic coefficients.

Ice accretion prediction involves complex physics comprising aerodynamics, heat transfer and multiphase flow, which are all time dependent and involve geometric deformation. The numerical method employed in this study predicts the ice accretion on aerodynamic surfaces as a result of water droplets hitting on the surface iteratively. It employs the general methodology for the simulation of ice accretion on airfoils, which is based on the successive calculation of air flow, water droplet trajectories, collection efficiency, heat transfer balance and accreted ice. In order to determine the flow field velocity components for droplet trajectory calculations, Hess-Smith panel method is used. Droplet trajectories are computed by using a Langrangian approach to obtain the collection efficiency distribution around the airfoil. To determine the thickness of ice, convective heat transfer coefficients are determined by using the two-dimensional Integral Boundary Layer equation and the thermodynamic balance is achieved with the Extended Messinger model. Extended Messinger Model is governed by four equations; energy equations in ice and water layers, a mass balance and a phase change or Stefan condition at the ice/water interface [Myers , 2001].

$$\frac{\partial T}{\partial t} = \frac{k_i}{\rho_i Cp_i}\frac{\partial^2 T}{\partial y^2} \tag{1}$$

$$\frac{\partial \theta}{\partial t} = \frac{k_w}{\rho_w Cp_w}\frac{\partial^2 \theta}{\partial y^2} \tag{2}$$

$$\rho_i \frac{\partial B}{\partial t} + \rho_w \frac{\partial h}{\partial t} = \rho_a \beta V_\infty \tag{3}$$

$$\rho_i L_F \frac{\partial B}{\partial t} = k_i \frac{\partial T}{\partial y} - k_w \frac{\partial \theta}{\partial y} \tag{4}$$

where θ and T are the temperatures, k_i and k_w are thermal conductives, Cp_i and Cp_w are the specific heats and h and B are the thickness of water and ice layers, respectively. In equation 3, $\rho_a \beta V_\infty$ is impinging water mass flow rates for a panel, respectively. Meanwhile, ρ_i and L_F refer the density of ice and the latent heat of solidification of water. In order to determine the ice and water thicknesses together with the temperature distribution at each layer, boundary and initial conditions must be specified. These are based on the following assumptions [Myers , 2001]:

- Ice is in perfect contact with the airfoil surface, which is taken to be equal to the air temperature, T_a:

$$T(0, t) = T_s \tag{5}$$

- The temperature is continuous at the ice/water boundary and is equal to the freezing temperature:

$$T(B, t) = \theta(B, t) = T_f \tag{6}$$

- At the air/water (glaze ice) or air/ice (rime ice) interface, heat flux is determined by convection (Q_c), radiation (Q_r), latent heat release (Q_l), cooling by incoming droplets (Q_d), heat brought in by runback water (Q_{in}), evaporation (Q_e) or sublimation (Q_s), aerodynamic heating(Q_a) and kinetic energy of incoming droplets (Q_k):

$$For\ glaze\ ice: \quad -k_w \frac{\partial \theta}{\partial y} = (Q_c + Q_e + Q_d + Q_r) - (Q_a + Q_k + Q_{in}) \ \ at\ y = B + h \tag{7}$$

$$For\ rime\ ice: \quad -k_i \frac{\partial T}{\partial y} = (Q_c + Q_s + Q_d + Q_r) - (Q_a + Q_k + Q_{in} + Q_l) \ \ at\ y = B \tag{8}$$

- Airfoil surface is initially clean:

$$B = h = 0, \quad t = 0 \tag{9}$$

Detailed information about this methodology can be found in References [Ozgen , 2008, 2010].

RESULTS AND DISCUSSION

Validation Case: Ice Accretion Prediction over NACA 0012 Wing Profile

The present method developed is first validated against the experimental and numerical studies over NACA 0012 airfoil performed by Wright et al. [Wright , 1997].

The geometric and flow conditions in the reference study are presented in Table 1.

Table 1: Geometric characteristics and flow conditions used in the calculations

Variables	Value
Ambient temperature, T_a	-27.8 °C
Freestream velocity, V_∞	58.1 m/s
Airfoil chord ,c	0.53 m
Liquid water content, ρ_a	1.3 g/m^3
Droplet diameter, d_p	20 μ m
Exposure time, t_{exp}	480 s
Ambient pressure, p_∞	95610 Pa
Angle of attack, α	4.0°
Humidity	100 %

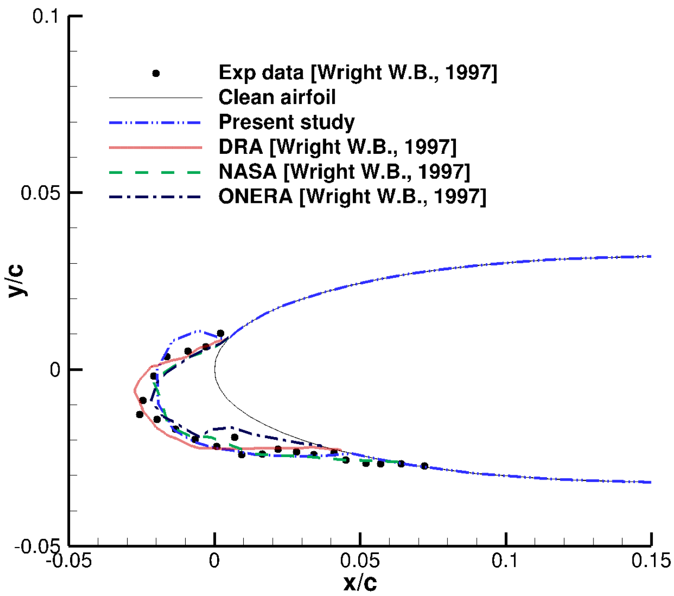

Figure 2: Comparison of ice shape predictions for NASA 27 case

In Figure 2, obtained ice shapes are compared with those obtained numerically by DRA, NASA and ONERA respectively. It is observed that all the predictions agree fairly well with the experimental data.

Effect of Panel Number on Ice Shape

In this case, the effect of panel number on ice shape is investigated with an arbitrary flow and geometry conditions. These parameters are given in Table 2.

In Figure 3 predicted ice shapes for NACA 0012 airfoil are presented for four different panel numbers. It is clearly seen that if the panel number is equal to 51, the predicted ice shape is signifacantly smaller than others, but ice shapes for 111, 121 and 154 spanwise panels look very similar. From these results, it is concluded that 121 spanwise panels is a good compromise between accuracy and speed so all the validation results that are presented below are for 121 spanwise panels.

Table 2: Parameters used to define icing profiles

Airfoils	NACA 0012
Chord	1.0 m
Angle of attack	4.7 °
Freestream velocity	25.7 m/s
Liquid water content, ρ_a	0.1 g/m^3
Droplet diameter, d_p	35 μ m
Ambient temperature, T_a	-6.0 °C
Exposure time, t_{exp}	10 hours
Ambient pressure, p_∞	95610 Pa
Humidity	100 %

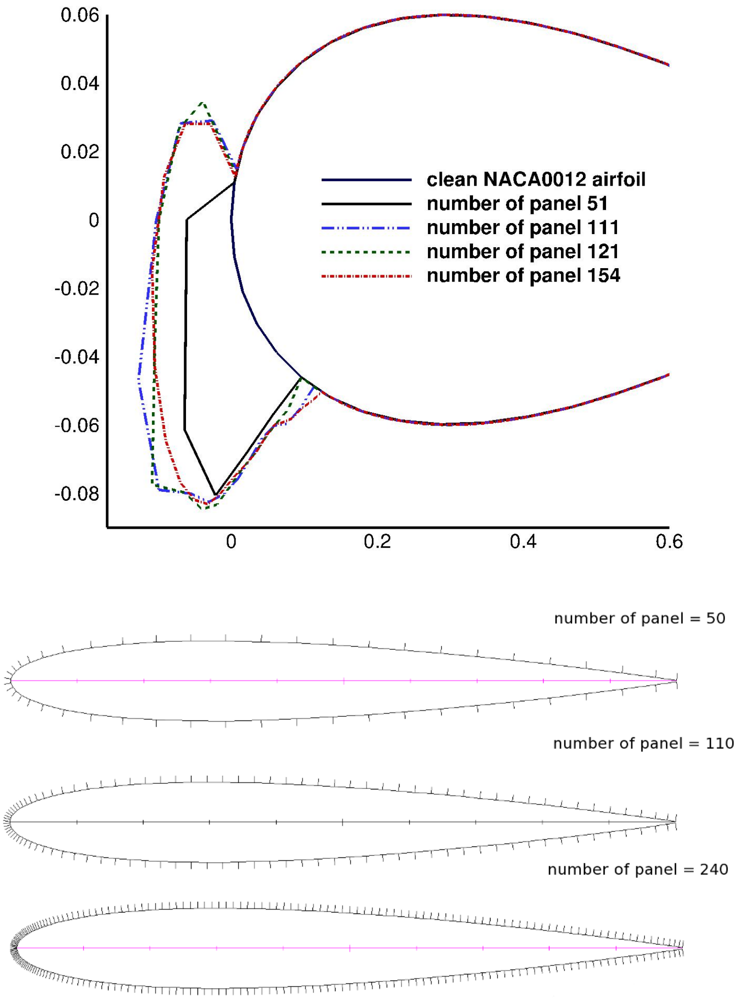

Figure 3: Predicted ice profiles for NACA 0012 airfoil for conditions in Table 2.

Effect of Temperature and Droplet Size on Ice Shape

In this case, a 5MW pitch controlled wind turbine blade profile (NACA 64618) was used to investigate the effects that atmospheric temperature and droplet size on ice accretion. The obtained results are compared against numerical study of Homola et al.[Homola , 2010]. The geometric and flow conditions in the reference study are presented in Table 3.

Table 3: Geometric characteristics and flow conditions used in the calculations

Airfoils	NACA 64618
Chord	1.9 m
Angle of attack	5 °
Relative air speed	25.7 m/s
Liquid water content, ρ_a	0.2 g/m^3
Droplet diameter, d_p	12, 17, 30 μ m
Ambient temperature, T_a	-2.5, -5, -7.5 °C
Exposure time, t_{exp}	120 minutes
Ambient pressure, p_∞	101300 Pa
Humidity	100 %

In Figure 5-6, obtained ice shapes are compared with those obtained numerically by Homola et al. (Turbice) respectively. It is observed that all the predictions agree fairly well with the numerical study of Homola et al.[Homola , 2010]. Present solver predicts bigger ice shape than homola et al. Atmospheric pressure, angle of attack, humidty, break up, splash effects are the information which are missing may cause this discrepancy.

Results in Figure 4 suggest that the ice shapes for $T_a =$ -5 °C and -7.5 °C are quite similar and exhibit rime ice characteristics. On the other hand, the ice shape obtained for $T_a =$ -2.5 °C is typically glaze and is significantly different than the other two. These results conform with expectations because rime ice typically occurs at low temperatures and low liquid water contents, which is what this test are precisely corresponds to for $T_a =$ -5 °C and -7.5 °C. However, $T_a =$ -2.5 °C is a significantly high temperature in terms of ice formation and hence yields a glaze ice shape.

It can be observed from the figures that as the droplet sizes increase, both the ice mass and the extent of iced region increases. Large droplets follow more ballistic trajectories resulting in a wider impingement zone and higher collection efficiencies. This results in wider and larger ice accretion as observed in Figure 5.

Ice Accretion Prediction on Wind Turbine Blade Profiles

Ice accretion prediction code was used to predict 2D ice profile shapes on the blade at three different span-wise locations for the Aeolos-H 30kW wind turbine under atmospheric icing conditions. Operating conditions shown in Table 4.

Predicted ice shapes for span-wise r/R = 0.15, 0.7 and 0.95 can be seen in Figure 6. The shape grows with increasing span due to the increasing sectional velocity and decreasing sectional chord length. Results show that the change caused by ice accretion degrads the aerodyanmic performance of the blade, especially near the tip section.

Table 4: Parameters used to define icing profiles

Airfoils	DU93-W-210
Root chord	0.703 m
Tip chord	0.02 m
Turbine diameter ,R	12 m
Liquid water content, ρ_a	0.1 g/m^3
Droplet diameter, d_p	35 μ m
Ambient temperature, T_a	-6.0 °C
Exposure time, t_{exp}	10 hours
Ambient pressure, p_∞	95610 Pa
Humidity	100 %

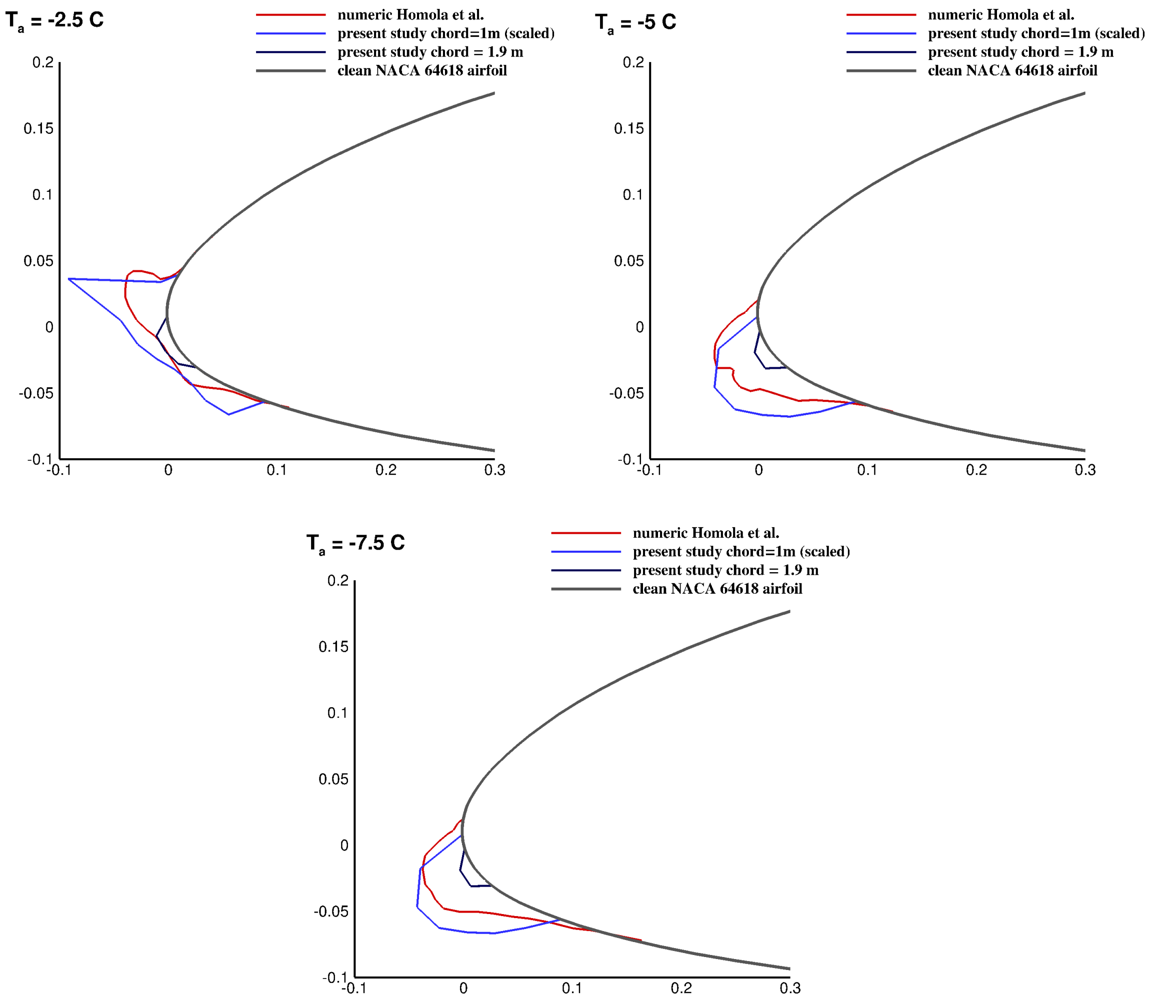

Figure 4: Predicted ice profiles for NACA 64618 airfoil for conditions in Table 3 (MVD = 17 μm).

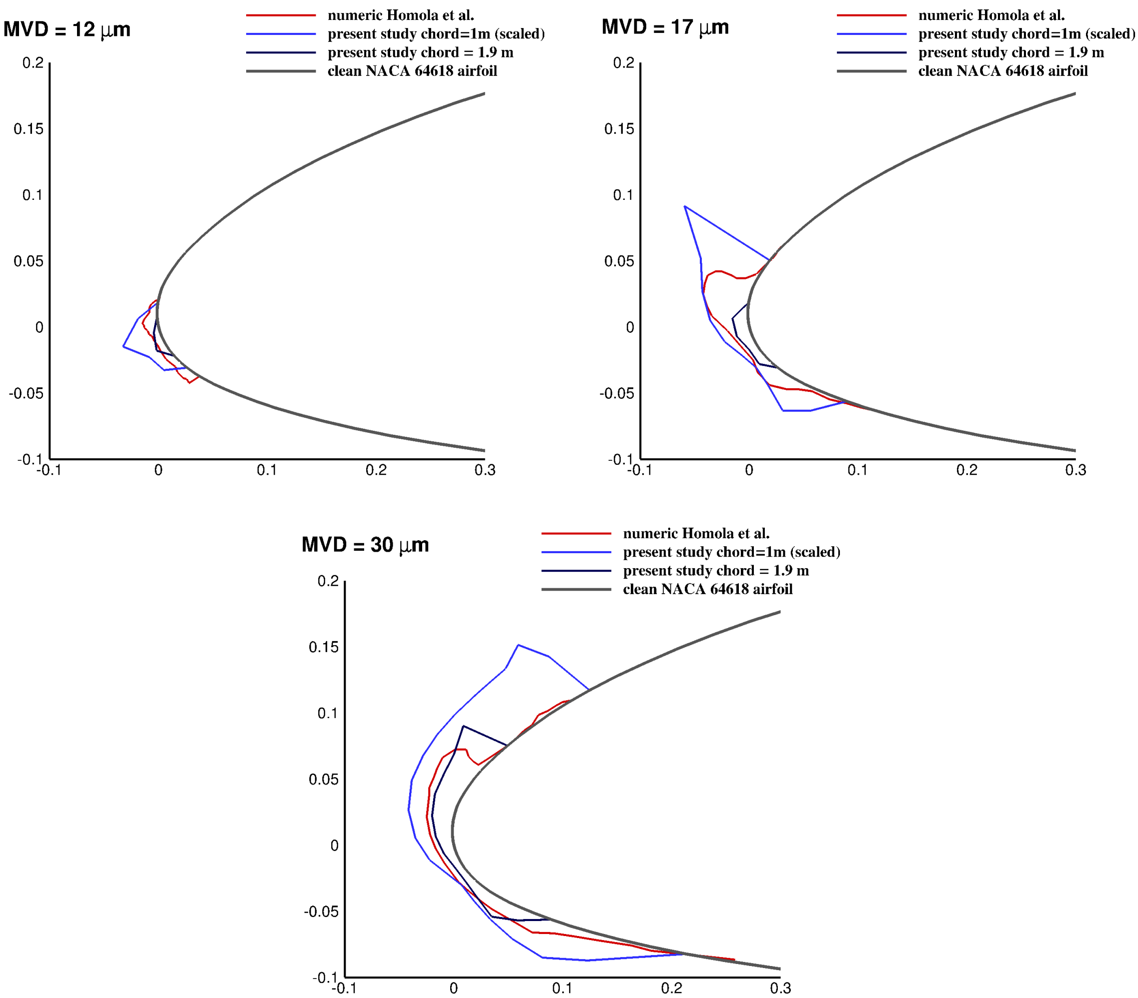

Figure 5: Predicted ice profiles for NACA 64618 airfoil for conditions in Table 3 (T_a = -2.5 °C).

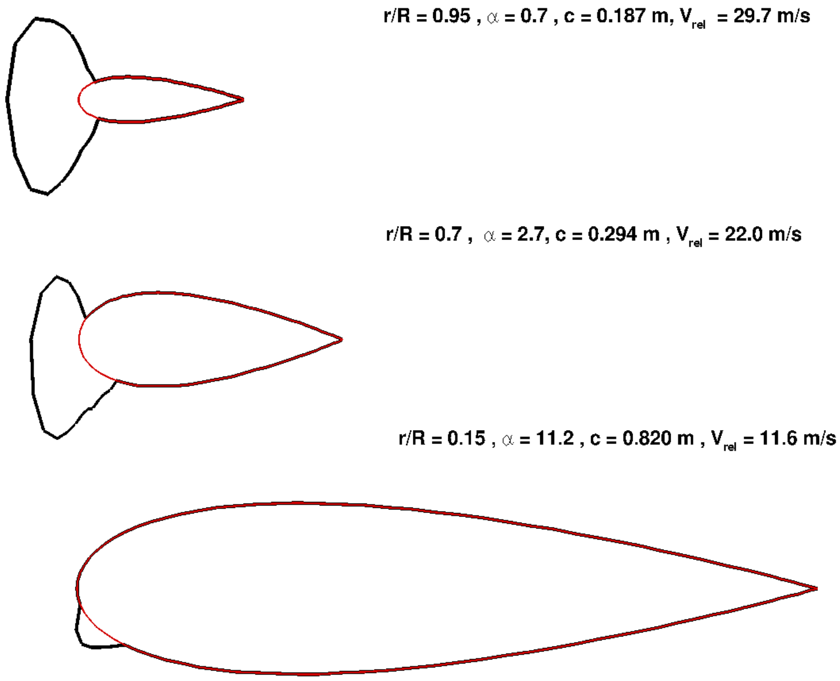

Figure 6: Predicted ice profiles at three span-wise locations for conditions in Table 4.

CONCLUSION

In this study, ice accretion on wind turbine blades is investigated under atmospheric icing conditions. Obtained preliminary results are analyzed and commented. Ice accretion code predicted ice shape on the blade sections rather well.

The results show that predicted ice shapes at low temperatures are quite similar and exhibit rime ice characteristics. These results conform with expectations since rime ice typically occurs at low temperatures and low liquid water contents while high temperature yields a glaze shape. It is seen that predicted ice shape grows with increasing span due to the increasing sectional velocity and decreasing sectional chord length. Results show that the change caused by ice accretion degraded the aerodynamic performance of the blade.

In the next step, ice accretion code will be coupled with BEM module to investigate aerodynamic performance losses in both rime and glaze ice conditions to estimate energy production losses of the wind turbines.

References

World Market Update 2013, Navigant Research, http://www.navigantresearch.com/research/world-market-update-2013, date of access April 23, 2015.

Jasinski, W.J. and Noe, S.C. and Selig, M.S. and Bragg, M.B. (1998) *Wind Turbine Performance Under Icing Conditions*, ASME, Vol.120, pp. 60-65, 1998

Talhaug L, Vindteknik K, Ronsten G, Horbaty R, Baring-Gould I, Lacroix A, et al., *Wind Energy Projects in Cold Climates*,1st ed. Executive Committee of the International Energy Agency Program for Research and Development on Wind Energy Conversion Systems; 2005; submitted for publication. p. 1–36, http://virtual.vtt.fi/virtual/arcticwind/reports/recommendations.pdf, date of access April 20, 2015.

Barber S., Wang Y., Jafari Y., Chokani N. and Abhari R. S., *The Impact of Ice Formation on Wind Turbine Performance and Aerodynamics*, Journal of Solar Energy Engineering, Vol.133/011007-1, February 2011.

Wind Energy in Cold Climates, IEA Wind *R, D&D* Task 19, http://arcticwind.vtt.fi/, date of access April 23, 2015.

Parent Oliver, Ilinca Adrian, *Anti-icing and De-icing Techniques for Wind Turbines: Critical Review*, Cold Regions Science and Technology, 65 (2011) 88-96.

Myers G. Tim,*Extension to the Messinger Model for Aircraft Icing*, AIAA JOURNAL, Vol. 39, No. 2, February 2001

Ozgen S., Canibek M., *Ice Accretion Simulation on Multi-Element Airfoils using Extended Messinger Model* ,Heat Mass Transfer, Volume 45, Issue 3, pp 305-322, 2008.

Ozgen S., Canibek M., *In Flight Icing Simulation with Supercooled Large Droplet Effects*,7th Int. Conference on Heat Transfer, Fluid Mechanics and Thermodynamics, Antalya, Turkey, 2010.

Wright WB, Gent RW, Guffond D., *Part II. Prediction of Airfoil Ice Accretion*, DRA/NASA/ONERA Collaboration on icing research, NASA CR-202349, 1997

Homola C.M., Virk S.M.,Wallenius T., Nicklasson P.J., *Sundsbϕ* S.A, *Effect of Atmospheric Temperature and Droplet Size Variation on Ice Accretion of Wind Turbine Blades*, J. Wind Eng. Ind. Aerodyn. (2010), doi:10.1016/j.jweia.2010.06.007